

## REPORT

## PROTEIN DESIGN

## Optical control of cell signaling by single-chain photoswitchable kinases

Xin X. Zhou,<sup>1</sup> Linlin Z. Fan,<sup>1\*</sup> Pengpeng Li,<sup>2†</sup> Kang Shen,<sup>2</sup> Michael Z. Lin<sup>1,3,‡</sup>

Protein kinases transduce signals to regulate a wide array of cellular functions in eukaryotes. A generalizable method for optical control of kinases would enable fine spatiotemporal interrogation or manipulation of these various functions. We report the design and application of single-chain cofactor-free kinases with photoswitchable activity. We engineered a dimeric protein, pdDronpa, that dissociates in cyan light and reassociates in violet light. Attaching two pdDronpa domains at rationally selected locations in the kinase domain, we created the photoswitchable kinases psRaf1, psMEK1, psMEK2, and psCDK5. Using these photoswitchable kinases, we established an all-optical cell-based assay for screening inhibitors, uncovered a direct and rapid inhibitory feedback loop from ERK to MEK1, and mediated developmental changes and synaptic vesicle transport in vivo using light.

**K**inase-mediated phosphorylation of serine, threonine, and tyrosine residues is a widespread mechanism of protein regulation, occurring on 40% of eukaryotic proteins (1). Because downstream responses often depend on the location, amplitude, and duration of protein phosphorylation (2, 3), methods to control kinases in space and time would aid in understanding signal transduction input-output relationships and in predicting the therapeutic utility of kinase modulation in disease. Optical control of protein activity can achieve high spatiotemporal resolution that would not be possible with pharmacological or conventional genetic methods. A variety of natural photosensory domains have been used to achieve optical control of protein activity via relocalization (4–12), sequestration (13, 14), fragment complementation (7, 15), induced avidity or concentration (16–18), or allostery (19–23). Optical activation of certain serine/threonine/tyrosine kinases has been achieved by relocalization to the plasma membrane (fig. S1A) and of certain receptor tyrosine kinases by clustering (fig. S1B) (24–29). Optical inhibition of kinases has also recently been reported (fig. S1C) (19). However, a generalizable design for single-chain light-activatable kinases that can function regardless of subcellular location has not previously been described.

To link optical inputs with kinase activity, we envisioned modular single-chain protein architectures that undergo large conformational changes in response to light. We hypothesized that we

could genetically attach dimerizing domains at two locations flanking a kinase active site so that the intramolecular dimer would sterically hinder substrate access at baseline, thereby caging the kinase. If the dimerizing domains were photodissociable, then illumination would convert the polypeptide into an open conformation and induce kinase activity (fig. S1D). As no natural dimeric domains are dissociated by visible light, we engineered one from the photodissociable tetrameric green fluorescent protein (FP) Dronpa145N (30). By rationally introducing mutations to break the antiparallel dimer interface, strengthen the cross-dimer interface in Dronpa145N, and improve maturation, we created a photodissociable dimeric Dronpa domain, pdDronpa1 (supplementary text and figs. S2 and S3). Like its parent Dronpa145N, pdDronpa1 was photodissociated and its fluorescence switched off by 500-nm cyan light, and photoassociated and its fluorescence restored by 400-nm violet light (Fig. 1A). Conveniently, pdDronpa1 was brighter than Dronpa145N in mammalian cells (fig. S4A) but required less light for off-photoswitching (fig. S4B). Fusion of two copies of pdDronpa1 to a protein of interest also caused less aggregation in cells than did Dronpa145N (fig. S4C). pdDronpa1 has a dissociation constant ( $K_d$ ) of 4.0  $\mu$ M as measured by analytical ultracentrifugation (table S2), making it suitable for intramolecular dimerization (31).

We set out to create single-chain optically controllable MEK1 using pdDronpa1 domains. The Raf-MEK-ERK signaling pathway plays vital roles in cell proliferation, differentiation, apoptosis, and migration (32), with cellular outcomes depending strongly on the dynamics of activation (33–35). Although Raf1 and the upstream activator Sos can be optically regulated via light-induced membrane recruitment (25, 26), this is not suitable for controlling MEK, which is pri-

marily localized to the cytosol regardless of pathway activity (36). To create a light-induced MEK, we first determined locations where insertion of pdDronpa domains could cage activity in the nonilluminated dimerized state. In addition to fusion at a terminus of the kinase, insertion of pdDronpa within the kinase domain should be possible, as the N terminus (NT) and C terminus (CT) of pdDronpa are located near each other. We identified the FG loop in MEK1, located across the active site from the MEK1 NT (37), as a favorable insertion point for pdDronpa (Fig. 1B). We thus explored caging MEK1 activity by fusing one pdDronpa1 domain at the kinase domain NT and a second one in the FG loop.

We first verified that attachment of monomeric FP domains at these two locations did not abolish MEK1 activity. A fusion of a single monomeric Dronpa domain at the NT of a constitutively active and minimized MEK1 kinase domain [active( $\Delta$ NT)MEK1], comprising amino acids 61 to 393 with Ser<sup>218</sup>  $\rightarrow$  Asp (S218D) and Ser<sup>222</sup>  $\rightarrow$  Asp (S222D) phosphomimetic mutations but lacking the flexible N-terminal substrate-binding domain (fig. S5A), drove phosphorylation of ERK independent of light, as expected (fig. S5B). Constructs with monomeric Dronpa inserted at various FG loop positions between amino acids 298 and 305 were also fully active (fig. S5C). Finally, active( $\Delta$ NT)MEK1 with enhanced green fluorescent protein (EGFP) fused to the NT and monomeric Dronpa inserted at amino acid 304 produced levels of phosphorylated ERK (pERK) comparable to that of active( $\Delta$ NT)MEK1 alone (fig. S5D); this result confirmed that MEK1 retains activity with non-dimerizing FP domains fused at the NT and in the FG loop.

We next tested whether active( $\Delta$ NT)MEK1 bearing dimerizing domains at the NT and in the FG loop would be caged at baseline. Indeed, attachment of pdDronpa1 domains at the NT and at amino acid 304 [creating proto-photoswitchable( $\Delta$ NT)MEK1, or proto-ps( $\Delta$ NT)MEK1] completely caged MEK1 activity to levels comparable to catalytically inactive MEK1 (fig. S5D). Other insertion points in the FG loop also allowed efficient caging (fig. S5E). We then tested the ability of proto-ps( $\Delta$ NT)MEK1 to be regulated by light. Illumination of cells expressing proto-ps( $\Delta$ NT)MEK1 induced pERK (fig. S5F). However, induced pERK levels were low relative to those produced by active( $\Delta$ NT)MEK1. Optical induction was enhanced by introducing an Asn<sup>145</sup>  $\rightarrow$  Lys (N145K) mutation in the second pdDronpa1, creating ps( $\Delta$ NT)MEK1. However, ps( $\Delta$ NT)MEK1 after photoinduction was still less active than unfused active( $\Delta$ NT)MEK1 on ERK (fig. S5F).

In full-length MEK1, amino acids 1 to 60 contain a substrate docking site that enhances affinity for ERK by a factor of 5 to 10 (38). Restoring this sequence to the NT of proto-ps( $\Delta$ NT)MEK1 increased both basal and induced activity (fig. S5G). When we introduced Val<sup>158</sup>  $\rightarrow$  Ile mutations into the pdDronpa1 domains to strengthen hydrophobic contacts at the dimeric interface, creating pdDronpa1.2 (fig. S5H), basal activity was

<sup>1</sup>Department of Bioengineering, Stanford University, Stanford, CA, USA. <sup>2</sup>Howard Hughes Medical Institute and Department of Biology, Stanford University, Stanford, CA, USA. <sup>3</sup>Department of Neurobiology, Stanford University, Stanford, CA, USA.

\*Present address: Program in Chemical Biology, Harvard University, Cambridge, MA, USA. †Present address: Boston Children's Hospital, Harvard Medical School, Boston, MA, USA. ‡Corresponding author. Email: mzl@stanford.edu

reduced while robust light responsiveness was maintained (fig. S5G). Maximal photoinduced pERK levels with this construct, designated photoswitchable MEK1 (psMEK1), were higher than with 20% serum stimulation (Fig. 1C). Basal ERK phosphorylation was further suppressed by reducing the length of the N-terminal linker, as expected for a steric caging mechanism, creating psMEK1tight (Fig. 1C). Topologically, psMEK1 and psMEK1tight can be considered full-length constitutively active forms of MEK1 with insertions of pdDronpa1.2 before amino acids 61 and 305 (fig. S6, A and B).

We investigated whether our approach could be generalized to other serine/threonine kinases, which all share a similar three-dimensional structure (39). We first ported the psMEK1 design to the closely related MEK2 (85% identical in the kinase domain; Fig. 1D). Replacing the constitutively active MEK1 sequences in psMEK1 with homologous sequences from constitutively

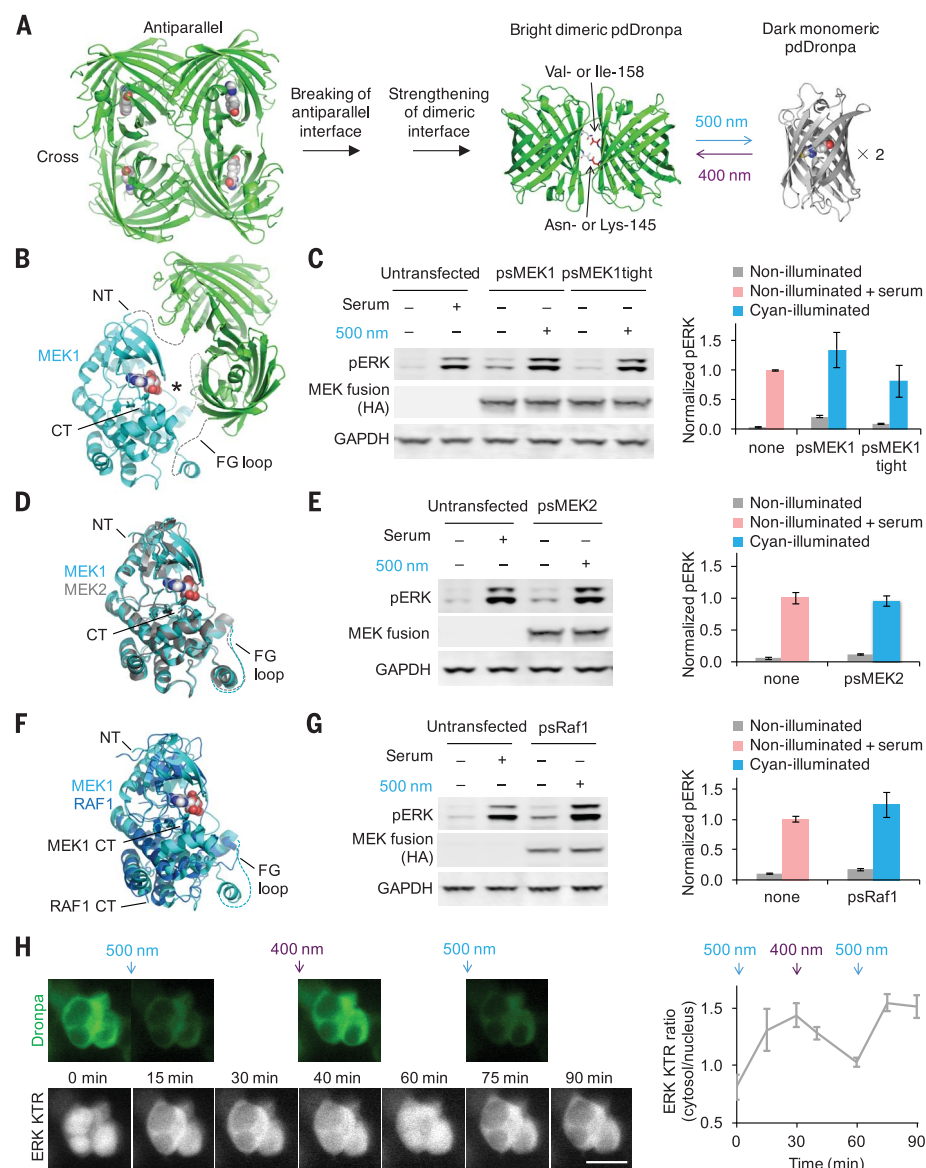
active MEK2 (fig. S6C) produced a robust photoswitchable MEK2 (psMEK2) that mediated light-induced ERK phosphorylation to levels similar to serum stimulation without further optimization (Fig. 1E). The photoswitchable kinase design thus appears easily generalizable within the same kinase family. We next attempted to construct a photoswitchable variant of Raf1, the kinase immediately upstream of MEK1, which is only 22% identical in the kinase domain (Fig. 1F). Previous studies have found that membrane targeting is sufficient for Raf1 activation (40). To create photoswitchable Raf1 (psRaf1), we appended a CAAX signal to the CT of the wild-type Raf1 kinase domain and attached pdDronpa1 and pdDronpa1 K145 at sites homologous to those in psMEK1 (fig. S6D). Cyan-illuminated psRaf1 induced pERK to levels similar to serum stimulation, whereas basal activity was comparable to that of untransfected cells (Fig. 1G). Thus, the photoswitch-

able kinase design is generalizable to multiple kinases.

Optical control allows spatiotemporal precision in induction, but in the case of our photoswitchable kinases, the ability to restore pdDronpa dimerization with violet light may allow recaging and thereby precise termination of kinase activity as well. Using psMEK1 and a translocation reporter of ERK phosphorylation, ERK KTR-mRuby2 (41), we demonstrated that photoswitchable kinases enable dosable and spatiotemporal control of biochemical events (supplementary text and figs. S7 and S8). psMEK1 did not produce detectable pathway output when expressed at moderate levels without illumination (supplementary text and fig. S8). We also found that the effects of psMEK1 could be rapidly reversed with violet light, enabling multiple rounds of kinase activation and inactivation (Fig. 1H). Finally, we tested whether photoswitchable kinases induced effects similar to those of the native kinases, and found that Dronpa

### Fig. 1. A modular and generalizable design for photoswitchable kinases.

(A) Photodissociable dimeric Dronpa (pdDronpa) variants were engineered from tetrameric DronpaN145. Residues 145 and 158 were further mutated to tune affinity. (B) Structural model of ps( $\Delta$ NT)MEK1 in the pre-illuminated state, showing the MEK1 core kinase domain with active site (asterisk) caged by pdDronpa1 domains attached at the NT and the FG loop (rendering based on PDB files 1S9J for MEK1 and 2Z6Y for Dronpa). Note that ps( $\Delta$ NT)MEK1 contains constitutively activating mutations as well. (C) Light-dependent induction of ERK phosphorylation (pERK) by psMEK1 and psMEK1tight. (D) Structural alignment of MEK1 (PDB 1S9J) with MEK2 (PDB 1S9I). (E) Light-dependent induction of pERK by psMEK2. (F) Structural alignment of MEK1 (PDB 1S9J) with Raf1 (PDB 3MOV). (G) Light-dependent induction of pERK by psRaf1. Note that psRaf1 contains a C-terminal CAAX motif for constitutive membrane localization. In (C), (E), and (G), cells were illuminated by cyan light at 20 mW/cm<sup>2</sup> for 2 min. Protein was detected via an N-terminal hemagglutinin (HA) tag, and lysate loading was monitored by blotting for glyceraldehyde-3-phosphate dehydrogenase (GAPDH). Serum stimulation durations were 5 to 10 min. Error bars denote SEM;  $n = 3$ . (H) psMEK1 activation can be temporally and reversibly controlled. Upper panels: Intrinsic pdDronpa fluorescence in psMEK1. Lower panels: mRuby2 fluorescence of the ERK KTR sensor. Cells were illuminated with cyan light at 200 mW/cm<sup>2</sup> for 1 min after the 0- and 60-min time points, and with violet light at 200 mW/cm<sup>2</sup> violet light for 3 s after the 30-min time point. pdDronpa fluorescence was imaged immediately after each light stimulation. Scale bar, 20  $\mu$ m. The graph shows quantification of cytosolic/nuclear KTR fluorescence over time. Error bars represent SEM of imaged cells.



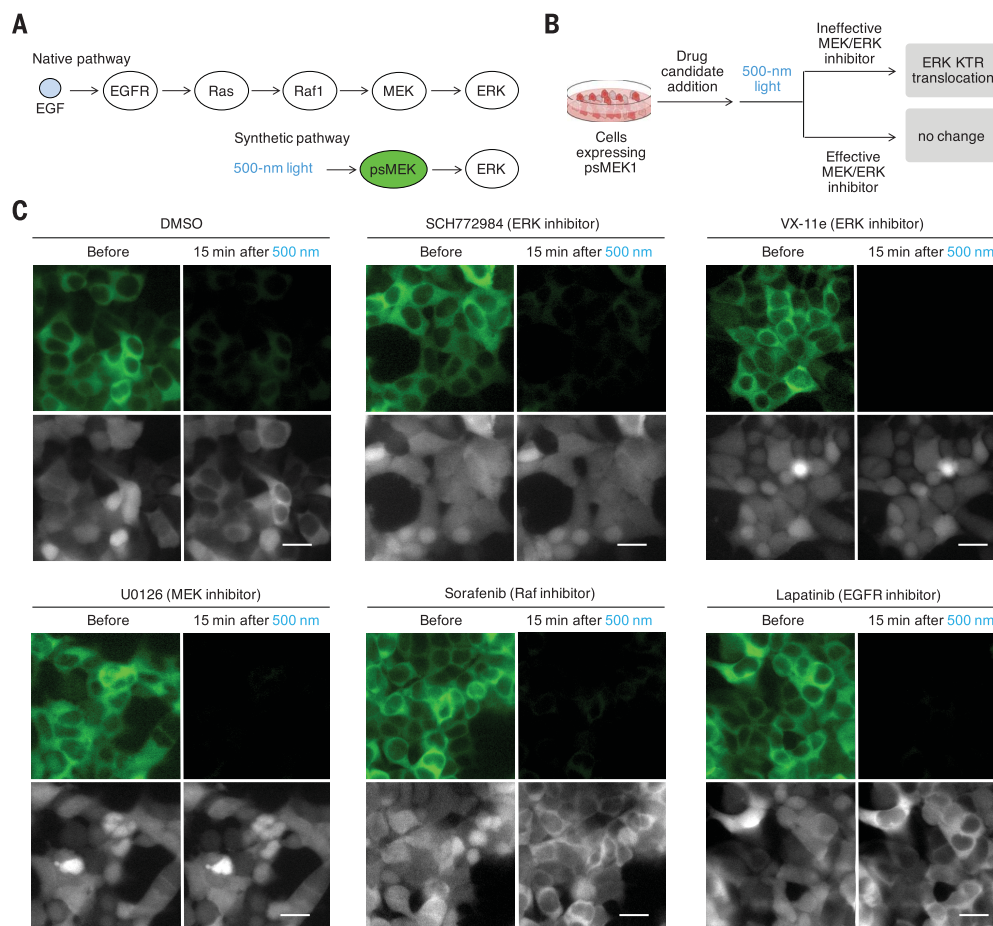


**Fig. 2. Cells expressing psMEK1 and the ERK KTR sensor enable all-optical cell-based assay for MEK and ERK inhibitors.** (A) In the native pathway, the chemical ligand EGF activates the receptor kinase EGFR, which then activates Ras. Activated Ras binds and activates Raf-1, which leads to MEK activation. In the synthetic pathway, psMEK1 is solely controlled by light and no longer responds to upstream activations. (B) Proposed all-optical cell-based assay for MEK and ERK inhibitors. Cells expressing psMEK1-P2A-ERK KTR-mRuby2 would be first incubated with drug candidates and then stimulated with light. The distribution of ERK KTR-mRuby2 would be monitored

to determine whether light could induce ERK phosphorylation in the presence of the drug. (C) The assay allowed determination of inhibitors specifically targeting MEK and ERK. Upper panels: Cyan light stimulation at 200 mW/cm<sup>2</sup> for 1 min switched off pdDronpa fluorescence. Lower panels: ERK KTR-mRuby2 translocation was monitored. Cells incubated with the ERK inhibitors SCH772984 or VX-11e, or with the MEK inhibitor U0126, did not show ERK KTR-mRuby2 translocation in response to psMEK1 activation, but cells incubated with dimethyl sulfoxide (DMSO) or inhibitors against upstream MEK activators Raf1 or EGFR (sorafenib and lapatinib, respectively) showed ERK KTR. Scale bars, 20 μm.

fusions did not affect kinase activation, kinetics, pathway dynamics, or substrate specificity (supplementary text and fig. S9).

The ability to control kinase activity with light and the availability of optical reporters such as ERK KTR suggests an all-optical method for kinase inhibitor screening, which would offer certain advantages. Photoinduction would be specific to the introduced photoswitchable kinase, whereas serum or growth factor stimulation would activate multiple pathways. By bypassing upstream steps (Fig. 2A), photoinduction enables screening for inhibitors specific for particular downstream steps. Furthermore, the timing of imaging can be optimized to identify inhibitors with immediate rather than delayed effects. We devised a screening procedure in which cells stably expressing psMEK1 and ERK KTR-mRuby2 were incubated with drug candidates and then stimulated by cyan light during time-lapse micros-

copy of ERK KTR (Fig. 2B). Effective inhibitors were expected to block light-induced ERK KTR translocation. Testing the ERK inhibitors SCH772984 and VX-11e and the MEK inhibitor U0126, we found that all three inhibitors prevented light-induced KTR translocation as expected (Fig. 2C). Inhibitors against the upstream proteins Raf1 and EGFR did not block the light-induced ERK phosphorylation (Fig. 2C), also as desired. These results demonstrated that all-optical kinase assays can allow the identification of inhibitors specifically against MEK or ERK, kinases of current clinical interest (42, 43). This concept should be adaptable to other kinases for which photoswitchable variants can be made.

We next used the photoswitchable kinases to investigate negative feedback in the Raf-MEK-ERK pathway. We observed that illumination of psRaf1 induced pERK, peaking at 2 min and then decaying (fig. S10A). Seeking to understand the mechanism

of this rapid down-regulation, we first asked whether down-regulation occurred only at the level of ERK or upstream of it. The activation loop in psMEK1 contains phosphomimetic sites to render the kinase domain constitutively active, so psMEK1 cannot be down-regulated by dephosphorylation. Thus, photoinduction of psMEK1 can specifically test for the presence of negative feedback directly on ERK. We found that increasing activation of psMEK1 resulted in increasing pERK in a nearly linear fashion (fig. S10B), which suggests that down-regulation of pERK after psRaf1 photoinduction occurred upstream of ERK, at the level of psRaf1 or endogenous MEK1/2.

We asked whether psRaf1 photoinduction causes biphasic activation and down-regulation of endogenous MEK1/2. To separate Raf1 activity and downstream feedback events in time, we took advantage of the bidirectionally photoswitchable nature of psRaf1 to create a short pulse

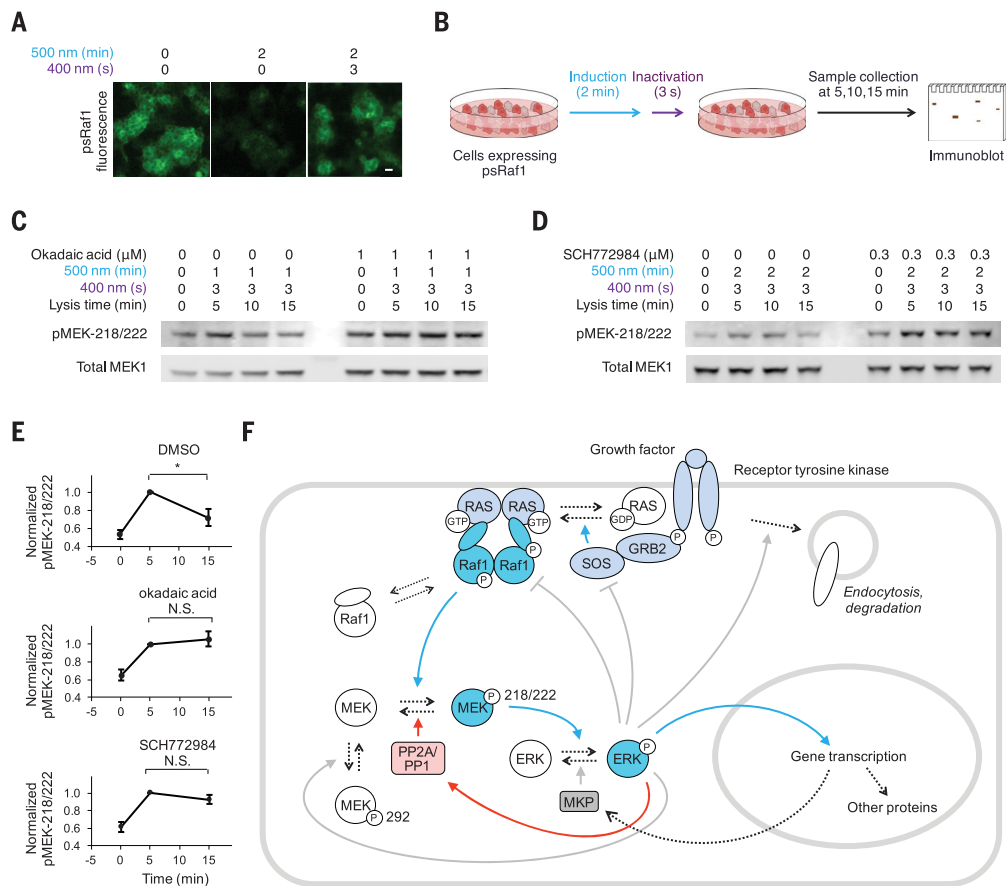


**Fig. 3. Photoswitchable kinases allow fine dissection of Raf-MEK signaling and identification of a novel fast feedback mechanism.** (A) Illumination with 500-nm light at 20 mW/cm<sup>2</sup> for 2 min effectively switched off pdDronpa fluorescence; illumination with 400-nm light at 10 mW/cm<sup>2</sup> for 3 s fully recovered pdDronpa fluorescence. Scale bar, 20 μm. (B) Cells stably expressing psRaf1 were illuminated by 500-nm light for 1 to 2 min, then illuminated with 400-nm light. Cell were then collected at 5, 10, and 15 min and immunoblotted. (C) MEK phosphorylation is down-regulated over time, and down-regulation requires PP2A/PP1. Lysis time is the time from the start of the stimulation to cell lysis. (D) MEK phosphorylation is down-regulated over time, and down-regulation requires ERK activity. Lanes 1 to 4: Decreases of pMEK-218/222 occurred over time after transient activation of psRaf1 (by

exposure to 500-nm light for 1 to 2 min followed by 400-nm light for 3 s), hence dephosphorylation of pMEK-218/222 occurs. Lanes 5 to 8: Down-regulation of pMEK did not occur in cells incubated with the ERK inhibitor SCH772984, indicating that ERK regulates the phosphatase activity. (E) Quantification of pMEK-218/222 over time in cells treated with DMSO, okadaic acid, or SCH772984. Error bars denote SEM; *n* = 3. \**P* < 0.05; N.S., not significant. Unpaired two-sided *t* tests were used for statistical analysis. (F) Simplified diagram of known positive (blue arrows) and negative (gray arrows) regulatory pathways mediating signaling from growth factor receptors to ERK. The new proposed pathway of ERK-induced dephosphorylation of pMEK-218/222 is marked with red arrows. Dashed arrows indicate protein transitions; solid arrows indicate regulatory effects.

of Raf1 activity. We verified that psRaf1 fluorescence was effectively switched off by a 2-min pulse of 500-nm light at 20 mW/cm<sup>2</sup> and fully recovered by 3 s of 400-nm light at 10 mW/cm<sup>2</sup> (Fig. 3A). We performed a pulse of photoinduction of psRaf1 using these conditions, then collected samples over time to track the fate of MEK1/2 phosphorylated at activating sites 218 and 222 (pMEK-218/222) during the cyan light pulse (Fig. 3B). pMEK-218/222 was down-regulated at later times (Fig. 3, C to E), confirming that psRaf1 photoinduction led to negative feedback on endogenous MEK1/2.

As psRaf1 was recycled after the cyan pulse period, the pMEK-218/222 signal at all time points assayed was generated during the pulse. Thus, the reduced levels of pMEK-218/222 at later time points could not have been due to down-regulation of psRaf1 at these later times,

but instead must have been due to a phosphatase acting on the pMEK-218/222 produced during the pulse. The PP1/PP2A inhibitor okadaic acid blocked negative feedback on pMEK-218/222 after pulsed psRaf1 photoinduction (Fig. 3, C and E); this finding suggests that the responsible phosphatase was PP1 or PP2A, which has been suggested to dephosphorylate MEK1/2 (44). Finally, we asked whether dephosphorylation was dependent on ERK activity. Indeed, down-regulation of pMEK-218/222 was blocked by the ERK inhibitor SCH772984 (Fig. 3, D and E). Taken together, these results indicate the existence a negative feedback pathway in which ERK induces PP1 or PP2A to dephosphorylate MEK1/2 at positions 218 and 222 (Fig. 3F), terminating further activation of ERK and subsequently allowing dephosphorylation of ERK by mitogen-activated protein kinase phosphatases

to dominate. Several mechanisms have been proposed to generate feedback inhibition in the Raf-MEK-ERK pathway, including endocytosis and degradation of tyrosine kinase receptors (2, 45), phosphorylation of regulatory sites (34, 42, 46), and transcriptional regulation of phosphatases (47). However, none of these reported mechanisms directly reverses the biochemical changes generated by pathway activation (Fig. 3F). Moreover, although PP1 or PP2A have been known to down-regulate the Raf-MEK-ERK pathway (42), it was unclear whether they are rapidly regulated by pathway activity. A major impediment to deciphering feedback inhibition was the inability of biochemical methods to create a short pulse of activity specific to the Raf-MEK-ERK cassette to observe time courses of down-regulation. We used the bidirectional photoswitchability of psRaf1 to create a pulse of activity, which revealed

that dephosphorylation of MEK at positions 218 and 222 by PPI or PP2A is induced by ERK (Fig. 3F). Adding to recent work with heterodimeric optobiochemical systems (25, 26), these findings highlight how the ability of photoswitchable proteins to create pulses of activity can be useful for kinetic assessment of downstream events.

Finally, we determined whether psRaf1 and psMEK1 can induce physiological effects in a

light-dependent manner in a living animal. In the roundworm *C. elegans*, the Raf-MEK-ERK pathway is activated by bacterial rectal infection to induce a protective tail-swelling response (48). We confirmed that expressing active( $\Delta$ NT)MEK1 and Raf1-CAAX constructs in hypodermis and gut cells induced tail swelling with 80% penetrance (Fig. 4A and fig. S11). We then asked whether ps( $\Delta$ NT)MEK1 or psRaf1 can induce these

effects in a light-dependent manner. Worms expressing ps( $\Delta$ NT)MEK1 or psRaf1 showed no or very low rates of tail swelling in the dark (0 or 2% penetrance, respectively), which suggests that the activities of ps( $\Delta$ NT)MEK1 and psRaf1 were well caged in vivo. In contrast, after exposure to low-intensity (0.7 mW/cm<sup>2</sup>) cyan light for 24 to 48 hours, worms expressing psMEK1 or psRaf1 exhibited tail swelling with 73% (psMEK1)

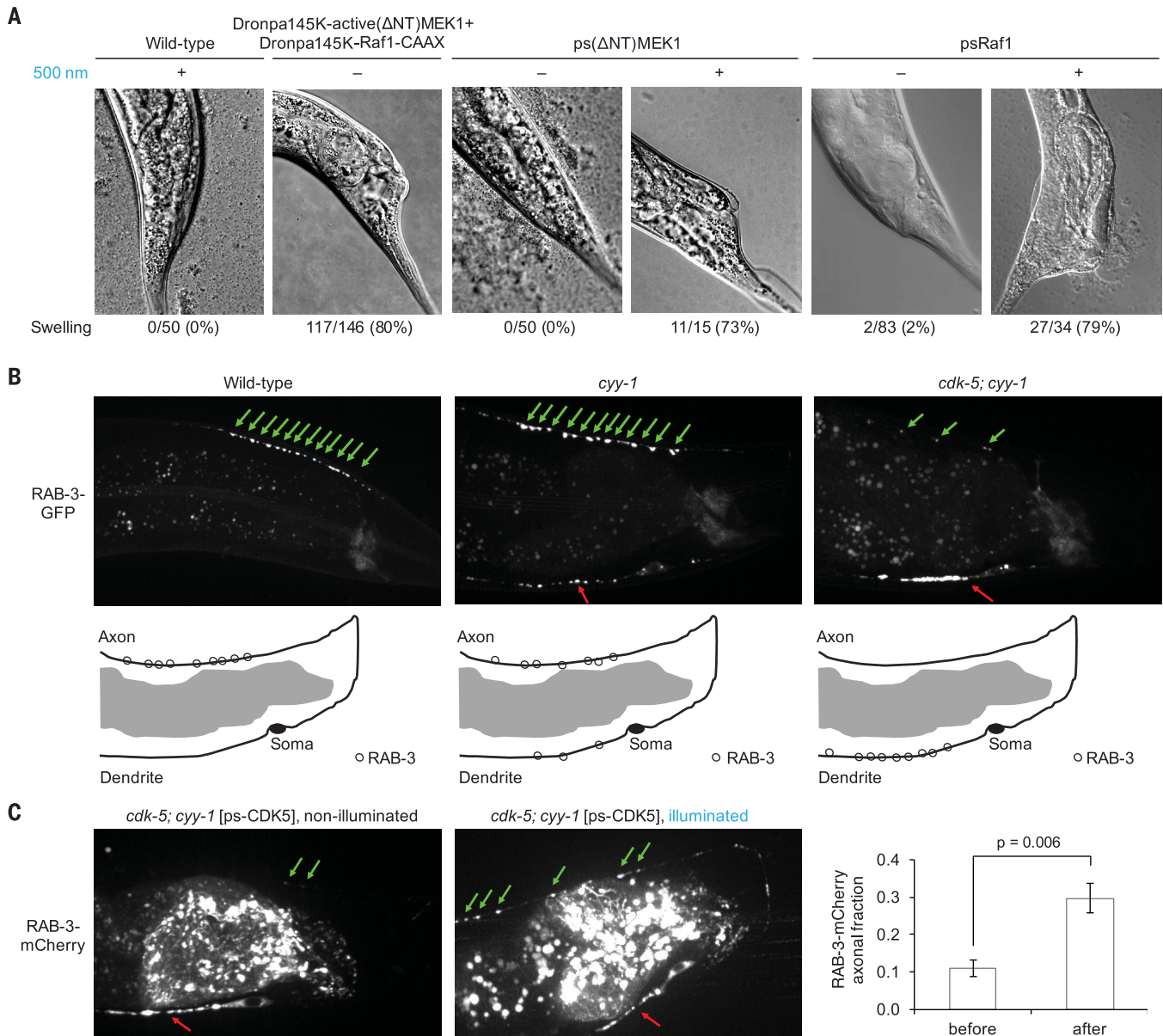


**Fig. 4. Optical control of kinase activity in living animals.** (A) Wild-type *C. elegans* worms showed no swollen tails even when grown in 500-nm light, whereas 80% of worms expressing Dronpa145K-active( $\Delta$ NT)MEK1 and Dronpa145K-Raf1-CAAX exhibited swollen tails in the dark ( $n = 146$ ). All worms expressing psMEK1 in the dark had normal tail shape ( $n = 50$ ), whereas 73% of worms expressing psMEK1 in cyan light showed tail swelling ( $n = 15$ ). Among worms expressing psRaf1, 98% had normal tail shape in the dark ( $n = 83$ ) and 79% showed tail swelling in light ( $n = 34$ ). (B) In wild-type worms, synaptic vesicles marked by RAB-3-GFP localize exclusively in the axon. In *cyy-1* mutants, RAB-3-GFP is partly mislocalized

to the dendrite. In *cyy-1; cdk-5* double-mutant worms, nearly all RAB-3-GFP localized to the dendrite. Green and red arrows mark vesicles located in the axon and dendrite, respectively. (C) Light-dependent restoration of CDK5 function in *cdk-5; cyy-1* worms. Nearly all RAB-3-mCherry in *cyy-1; cdk-5* worms expressing psCDK-5 localized in the dendrite in the absence of light ( $n = 11$ ), similar to *cyy-1; cdk-5* worms. Cyan illumination restored axonal localization of some vesicles ( $n = 10$ ), similar to the phenotype of *cyy-1* worms. The light effect was statistically significant ( $P = 0.006$ , unpaired two-sided  $t$  test). Error bars denote SEM. Worms were exposed to 400-nm light at 0.7 mW/cm<sup>2</sup> for 24 to 48 hours before imaging.

or 79% (psRaf1) penetrance ( $P < 0.0001$  compared to nonilluminated penetrance by two-sided Fisher's exact test). These results show that the psMEK1 and psRaf1 proteins enable optical control over the Raf-MEK-ERK pathway in a living animal.

To further demonstrate the generalizability of the photoswitchable kinase design and its ability to investigate protein in vivo, we created a photo-switchable cyclin-dependent kinase 5 (psCDK5) in the same manner as psMEK1 and psRaf1 (fig. S6E). In multiple animal species, CDK5 regulates the differentiation and maintenance of neuronal structures (49). In worms, loss of CDK5 enhances the phenotype of cyclin Y deficiency, in which synaptic vesicles mislocalize to the dendrite of the DA9 neuron (50). Specifically, *cyt-1;cdk-5* worms mislocalize nearly all vesicles to dendrites, whereas in *cyt-1* worms, only a fraction of vesicles are mislocalized (Fig. 4B). We hypothesized that *cyt-1;cdk-5* worms expressing psCDK5 would exhibit light-dependent restoration toward the *cyt-1* phenotype, in which the majority of vesicles are situated correctly in axons. We found that nearly all vesicles in psCDK5-expressing *cyt-1;cdk-5* worms distributed in the dendrite in the dark, as expected. After exposure of these worms to 24 hours of cyan light at  $0.7 \text{ mW/cm}^2$ , significantly more vesicles appeared in axons ( $P = 0.006$ , two-sided  $t$  test), resembling the phenotype of *cyt-1* worms (Fig. 4C). These results show that a photoswitchable kinase can recapitulate wild-type kinase functionality in the photoinduced state.

In addition to bidirectional photocontrol of activity, the autocatalytic and fluorescent chromophore of pdDronpa also allows independence from biochemical cofactor availability and enables self-reporting of the activation state. Only the testing of several linker lengths and pdDronpa affinity variants was required to create different light-regulated constructs. Our experience suggests a rational process for optimizing a photoswitchable variant for a given kinase of interest (fig. S12). Because all serine/threonine and tyrosine kinases have the same basic scaffold (39), our approach could potentially be applied to impart optical control to many kinases.

Our work also suggests that pdDronpa insertion may be a versatile method for optobiochemical control beyond kinases. Loops occur frequently near functional surfaces of proteins, as they serve

to link secondary structural elements. We found that pdDronpa domains can be inserted into loops of a protein of interest while preserving the functions of both pdDronpa and the protein. Thus, it may be possible to use pdDronpa to control the accessibility of many protein surfaces in a light-dependent manner.

## REFERENCES AND NOTES

- G. Manning, D. B. Whyte, R. Martinez, T. Hunter, S. Sudarsanam, *Science* **298**, 1912–1934 (2002).
- J. J. Bergeron, G. M. Di Guglielmo, S. Dahan, M. Dominguez, B. I. Posner, *Annu. Rev. Biochem.* **85**, 573–597 (2016).
- J. E. Purvis, G. Lahav, *Cell* **152**, 945–956 (2013).
- S. Shimizu-Sato, E. Huq, J. M. Tepperman, P. H. Quail, *Nat. Biotechnol.* **20**, 1041–1044 (2002).
- A. Levskaya, O. D. Weiner, W. A. Lim, C. A. Voigt, *Nature* **461**, 997–1001 (2009).
- M. Yazawa, A. M. Sadaghiani, B. Hsueh, R. E. Dolmetsch, *Nat. Biotechnol.* **27**, 941–945 (2009).
- M. J. Kennedy *et al.*, *Nat. Methods* **7**, 973–975 (2010).
- D. Strickland *et al.*, *Nat. Methods* **9**, 379–384 (2012).
- O. I. Lungu *et al.*, *Chem. Biol.* **19**, 507–517 (2012).
- R. P. Crefcoeur, R. Yin, R. Ulm, T. D. Halazonetis, *Nat. Commun.* **4**, 1779 (2013).
- K. Müller *et al.*, *Nucleic Acids Res.* **41**, e124 (2013).
- F. Kawano, H. Suzuki, A. Furuya, M. Sato, *Nat. Commun.* **6**, 6256 (2015).
- D. Chen, E. S. Gibson, M. J. Kennedy, *J. Cell Biol.* **201**, 631–640 (2013).
- S. Lee *et al.*, *Nat. Methods* **11**, 633–636 (2014).
- Y. Nihongaki, F. Kawano, T. Nakajima, M. Sato, *Nat. Biotechnol.* **33**, 755–760 (2015).
- X. Wang, X. Chen, Y. Yang, *Nat. Methods* **9**, 266–269 (2012).
- L. J. Bugaj, A. T. Choksi, C. K. Mesuda, R. S. Kane, D. V. Schaffer, *Nat. Methods* **10**, 249–252 (2013).
- L. B. Motta-Mena *et al.*, *Nat. Chem. Biol.* **10**, 196–202 (2014).
- O. Daglilan *et al.*, *Science* **354**, 1441–1444 (2016).
- C. Gasser *et al.*, *Proc. Natl. Acad. Sci. U.S.A.* **111**, 8803–8808 (2014).
- J. Lee *et al.*, *Science* **322**, 438–442 (2008).
- D. Strickland, K. Moffat, T. R. Sosnick, *Proc. Natl. Acad. Sci. U.S.A.* **105**, 10709–10714 (2008).
- Y. I. Wu *et al.*, *Nature* **461**, 104–108 (2009).
- S. Wend *et al.*, *ACS Synth. Biol.* **3**, 280–285 (2014).
- J. E. Toettcher, O. D. Weiner, W. A. Lim, *Cell* **155**, 1422–1434 (2013).
- K. Zhang *et al.*, *PLOS ONE* **9**, e92917 (2014).
- M. Grusch *et al.*, *EMBO J.* **33**, 1713–1726 (2014).
- K.-Y. Chang *et al.*, *Nat. Commun.* **5**, 4057 (2014).
- N. Kim *et al.*, *Chem. Biol.* **21**, 903–912 (2014).
- X. X. Zhou, H. K. Chung, A. J. Lam, M. Z. Lin, *Science* **338**, 810–814 (2012).
- T. H. Evers, E. M. van Dongen, A. C. Faesen, E. W. Meijer, M. Merx, *Biochemistry* **45**, 13183–13192 (2006).
- F. Chang *et al.*, *Leukemia* **17**, 1263–1293 (2003).
- J. G. Albeck, G. B. Mills, J. S. Brugge, *Mol. Cell* **49**, 249–261 (2013).
- S.-Y. Shin *et al.*, *J. Cell Sci.* **122**, 425–435 (2009).
- C. Cohen-Saidon, A. A. Cohen, A. Sigal, Y. Liron, U. Alon, *Mol. Cell* **36**, 885–893 (2009).

- C.-F. Zheng, K.-L. Guan, *J. Biol. Chem.* **269**, 19947–19952 (1994).
- J. F. Ohren *et al.*, *Nat. Struct. Mol. Biol.* **11**, 1192–1197 (2004).
- A. J. Bardwell, L. J. Flatauer, K. Matsukuma, J. Thorer, L. Bardwell, *J. Biol. Chem.* **276**, 10374–10386 (2001).
- J. A. Endicott, M. E. M. Noble, L. N. Johnson, *Annu. Rev. Biochem.* **81**, 587–613 (2012).
- J. Hu *et al.*, *Cell* **154**, 1036–1046 (2013).
- S. Regot, J. J. Hughey, B. T. Bajar, S. Carrasco, M. W. Covert, *Cell* **157**, 1724–1734 (2014).
- B. Cseh, E. Doma, M. Baccarini, *FEBS Lett.* **588**, 2398–2406 (2014).
- A. A. Samatar, P. I. Poulikakos, *Nat. Rev. Drug Discov.* **13**, 928–942 (2014).
- D. Bae, S. Ceryak, *Biochem. Biophys. Res. Commun.* **385**, 523–527 (2009).
- L. K. Goh, A. Sorkin, *Cold Spring Harb. Perspect. Biol.* **5**, a017459 (2013).
- F. Catalanotti *et al.*, *Nat. Struct. Mol. Biol.* **16**, 294–303 (2009).
- R. Fritsche-Guenther *et al.*, *Mol. Syst. Biol.* **7**, 489 (2011).
- H. R. Nicholas, J. Hodgkin, *Curr. Biol.* **14**, 1256–1261 (2004).
- R. Dhavan, L.-H. Tsai, *Nat. Rev. Mol. Cell Biol.* **2**, 749–759 (2001).
- C. Y. Ou *et al.*, *Cell* **141**, 846–858 (2010).

## ACKNOWLEDGMENTS

We thank G. Colakoglu for assistance with worm experiments; Y. Tao and L. Feng for assistance with crystallographic data collection and analysis; X. Liu and T. Fu for assistance with protein structure refinement; J. Philo for assistance with sedimentation equilibrium analysis; L. Tao and G. Colakoglu for assistance with the worm experiments; T. Kudo, S. Regot, and M. Covert for ERK KTR constructs; K. Zhang and B. Cui for the Raf1 plasmid; R. Tran, X. Bao, and P. Khavari for the MEK1 plasmid; M. Davidson for the Neptune1-fascin plasmid; and members of the Lin laboratory for valuable assistance with experiments and advice on the manuscript. Supported by a Stanford Graduate Fellowship and a HHMI International Graduate Student Fellowship (X.X.Z.), the Stanford School of Engineering Undergraduate Visiting Researcher Program (L.Z.F.), and NIH Pioneer Award 5DP1GM11003 (M.Z.L.). All data are available in the manuscript or supplementary materials. Author contributions: X.X.Z. designed and characterized light-inducible kinases, generated protein crystals, solved x-ray structures, performed worm experiments, engineered pdDronpa1 variants, and co-wrote the manuscript; L.Z.F. characterized light-inducible intersectin and designed and characterized pdDronpaV and pdDronpaM; P.L. performed worm transgenesis and imaging; K.S. provided advice and supervision on worm experiments; and M.Z.L. conceived experiments, provided advice, and co-wrote the manuscript. The authors declare no competing financial interests.

## SUPPLEMENTARY MATERIALS

www.sciencemag.org/content/355/6327/836/suppl/DC1  
Materials and Methods  
Figs. S1 to S12  
Tables S1 and S2  
Movie S1  
References (51–62)

23 June 2016; resubmitted 15 November 2016  
Accepted 23 January 2017  
10.1126/science.aah3605



## Optical control of cell signaling by single-chain photoswitchable kinases

Xin X. Zhou, Linlin Z. Fan, Pengpeng Li, Kang Shen, and Michael Z. Lin

*Science*, **355** (6327), .

DOI: 10.1126/science.aah3605

### Shining a light on cell signaling

Protein kinases are proteins that are used to transmit signals within cells. Zhou *et al.* engineered diverse kinases so that they could be switched on and off with visible light. They modified the fluorescent protein Dronpa so that instead of being tetrameric, it dimerized in violet light and dissociated in cyan light, and they fused two copies to representatives from different families of kinases. The engineered kinases could be photo-switched with spatial and temporal precision and were successfully used to study a variety of signaling pathways.

*Science*, this issue p. 836

### View the article online

<https://www.science.org/doi/10.1126/science.aah3605>

### Permissions

<https://www.science.org/help/reprints-and-permissions>

Use of this article is subject to the [Terms of service](#)

---

*Science* (ISSN 1095-9203) is published by the American Association for the Advancement of Science. 1200 New York Avenue NW, Washington, DC 20005. The title *Science* is a registered trademark of AAAS.  
Copyright © 2017, American Association for the Advancement of Science